

A New Interface Identification Technique Based on Absolute Density Gradient for Violent Flows

Yan Zhou and QW Ma*

School of Mathematics, Computer Science and Engineering, City University London
Northampton Square, London, EC1V 0HB

*Corresponding author email: q.ma@city.ac.uk

Abstract

An identification technique for sharp interface and penetrated isolated particles has been developed for simulating two-dimensional, incompressible and immiscible two-phase flows using meshless particle methods. This technique is based on the numerically computed density gradient of fluid particles and is intended to capture large interface deformation and even topological changes such as merging and breaking up of phases. A number of assumed particle configurations have been examined, including these with different level of randomness of particle distribution. The tests will show that the new technique can correctly identify almost all the interface and isolated particles, and also show that it is better than other existing popular methods tested.

1 Introduction

In numerical simulations of two-phase flows, the identification of interface is essential in solving equations describing the transport of momentum, mass and energy. There are various methods for interface identification which can be broadly divided into two groups. One is for mesh-based methods, usually based on an indicator function resulting in an interface with the thickness either covering several grid cells or one cell. The other group is for meshless-based methods, in which particles are moved in Lagrangian formulation, yielding an interface directly which is coincided with the position of a set of particles.

In mesh-based methods, the volume of fluid (VOF) method captures the interface by the indicator function formulated with a volume fraction of either phase. To represent a sharp interface within the mesh, the VOF is often complemented by reconstruction techniques such as piece wise constant approach(Hirt & Nichols 1981; Yokoi 2007), piecewise linear approach (Aulisa et al. 2007; Rudman 1997) in which the interface in a mesh is assumed to be a line in 2D or a plain in 3D, piecewise quadratic(Diwakar et al. 2009; Renardy & Renardy 2002)orpiecewise cubic spline(Ginzburg & Wittum 2001; López et al. 2004). To simplify the computational treatment, Rudman (1997), Ubbink & Issa (1999) and Xiao et al. (2005) employed another way to identify the interface by using a range of value of a volume fraction, which actually represent an interface covering several meshes. And later Weller (2008) and Hoang et al. (2013) introduced the artificial compression terms to sharpen the interface and counteract the numerical diffusion. Different from artificial geometric representation in the VOF when reconstructing the interface, the indicator in level-set method (Osher & Sethian 1988) is a smoothed signed distance function from the interface and zero level-set gives the location of the interface. To remedy its mass non-conservation problem, re-initialization for the signed distance function (Sussman & Fatemi 1999; Min 2010) and mass corrections (Ausas et al. 2011; Zhang et al. 2010) were widely adopted. Instead of using Eulerian mesh, the arbitrary Lagrangian-Eulerian mesh

system was also adopted in which the unstructured meshes are moved to keep the grid nodes at the interface (Muzaferija & Perić 1997; Tukovic & Jasak 2012).

As for meshless-based methods, the interface can be inherently tracked by moving particles which are initially allocated and remain as one phase during the simulation. For methods that solve two phases in one set of equations, such as in Hu & Adams (2007) and Chen et al. (2015) based on smoothed particle hydrodynamics (SPH) method and in Shakibaeinia & Jin (2012); Khayyer & Gotoh (2013) employing the Moving Particle Semi-implicit (MPS) method, interface conditions are implicitly implemented and thus the interface does not need to be explicitly identified. However, for explicit boundary condition implementation, two situations can be observed. One situation is that the flow is not violent or large deformations do not occur, under which particles on the free surface in single phase flows or on the interface of multiphase flows are maintained during the simulation (Ma 2005), in which the interface is known and its identification is not necessary. The other situation comes with flows being violent or with large deformations and therefore the inner and boundary particles are changeable (Lee et al. 2008; Ma & Zhou 2009; Shao 2012). In this situation, the interface particles and isolated particles (penetrating to the other phase) must be identified in every time step.

In this paper a new interface (and also isolated) particle identification technique is proposed for the meshless-based methods, which is based on absolute density gradient for violent flows. In the next section the existing methods for interface particle identification used in the meshless-based methods will be briefly reviewed. Then the formulations of the new identification technique and parameters tests are given, followed by the comparisons between the new technique and the existing ones. Finally, validations of the new technique on different density ratios, different degree of randomness of particle distribution, various sizes of the support domain in calculating the density gradient and different flow conditions will be carried out.

2 Brief review on surface or interface particle identification methods for meshless methods

Many applications of meshless methods (e.g. incompressible SPH (ISPH), MPS, MLPG) in single phase wave simulation depend strongly on free surface particle identification based on which the dynamic surface boundary condition can be implemented. A number of approaches have been proposed and adopted in various meshless methods, such as these using the particle number density method (abbreviated to PND) in MPS (Koshizuka et al. 1998; Gotoh & Sakai 2006; Xu & Jin 2014) and fluid density in ISPH (Shao 2009). Both techniques are developed mainly for single phase problems, which lead to lower particle number density (MPS) or lower density (SPH) on the free surface, satisfying Eq. (1) and Eq. (2), respectively

$$n_i < \theta n^0 \quad (1)$$

$$\rho_i < \kappa \rho^0 \quad (2)$$

where $n_i = \sum_j w(|\vec{r}_j - \vec{r}_i|)$ is the particle number density for the target particle i with w being a weight function and n^0 denotes the inner particle number density which is initially defined. Similar to particle number density, $\rho_i = \sum_j m_j w(|\vec{r}_j - \vec{r}_i|)$ is used to give the estimated density and ρ^0 denotes the specified density of fluid. θ and κ are coefficients to evaluate the decreasing of n_i and ρ_i for the

surface particles. As pointed by Koshizuka & Oka(1996) the value of θ could be in the range of 0.8 to 0.99 and was selected as 0.97 in their case study of dam breaking and in modelling weir flows (Xu & Jin 2014). n_i and κ were chosen as 0.95 for simulating breaking waves on slopes (Koshizuka et al. 1998) and 0.99 for simulating water entry of a free-fall object (Shao 2009). However, this simple approach has been found often to identify incorrectly the interface (or free surface) particles, especially when the particles are unevenly distributed.

As a supplementary to PND, a mixed particle number density and auxiliary function method (MPAM) was proposed (Ma & Zhou 2009) by additionally counting the existing surface particles and the occupied quarters and crossed rectangles in the support domain in Ma & Zhou (2009). Following Shao (2009) and Ma & Zhou (2009), the method was further developed by Zheng et al. (2014) by defining two quarter-dividing systems and counting the occupied ones in which the value of κ was chosen as 0.9. As confirmed by many calculations in the cited papers, the accuracy of identifying interface particles is significantly improved with the auxiliary functions. However apart from the complexity in sorting neighbouring particles into quarters and other specific regions, the dependence on the identification of the previous time step could lead to error accumulation once misidentification occurs in previous steps.

Lee et al. (2008) and Rafiee et al. (2012) employed a tracking method by estimating the divergence of position vector, \vec{r} , with the expression of

$$(\nabla \cdot \vec{r})_i \approx \sum_j \Delta V_j (\vec{r}_j - \vec{r}_i) \cdot \nabla w(|\vec{r}_j - \vec{r}_i|) \quad (3)$$

where ΔV_j is the volume of particle associated with particle j . The value of the numerical divergence from Eq. (3) is close to 2 for inner particles in two dimensional simulations and decreases on the free surface particles for the reason that the number of neighbouring particles is smaller and the support of the kernel is truncated. Thus the criterion identifying the free surface particles is set as

$$(\nabla \cdot \vec{r})_i < 1.5 \quad (4)$$

It was indicated that not all the surface particles were identified (Lee et al. 2008) and some inner particles are over identified (Lind et al. 2012) although the misjudgements appeared to be insignificant in the cases they have considered by using the method. Because the theoretical value of the position vector divergence should be 2 for both inner and surface particles, its numerical value should be close to 2 even near or on the interface if more accurate and consistent approximation, such as SFDI gradient scheme (Ma 2008) is employed to estimate the divergence. From this point of view, the method is questionable for its general use and so will not be considered further in this paper.

Above interface particle identification methods developed for single phase can be applied in a straightforward way to interface identification in two-phase flows by involving the particles of the other phase if the difference of the two phase densities are large (Shao et al 2012) or by neglecting the one phase and picking out the ‘surface’ of the rest phase. To improve the accuracy and reduce the complexity of the interface identification technique, a new approach based on the absolute density gradient is proposed in this paper. This method is based on the fact that the density gradient is infinite on the interface but zero away from it. In two-phase violent flows, it often happens that one phase penetrates into the other. In that case, the penetrated parts are usually represented by isolated particles for which special treatment are necessary (Gotoh & Sakai 2006). Gotoh & Sakai (2006) also provided an identification method using a combination of particle number density and the number of

neighbouring particles of the other phase. In comparison the newly proposed technique is able to identify such isolated particles in a more consistent way.

3 Absolute density gradient technique

For immiscible two-phase flows with the sharp density jump at the interface, the density gradients are 0 for inner particles and become theoretically infinite at the interface if both phases are incompressible. For weak compressible phases, the density gradients are close to 0 for inner particles and are also theoretically infinite at the interface. To utilize this fact for interface identification, the absolute value of density gradient is numerically computed as below

$$\beta = |\rho_{,x}| + |\rho_{,y}| \quad (5)$$

where

$$|\rho_{,d}| = \frac{2}{\sum_j w(\vec{r}_j - \vec{r}_i)} \sum_j |\rho_i - \rho_j| \frac{|r_{j,d} - r_{i,d}|}{\Delta r_{ij}^2} w(\vec{r}_j - \vec{r}_i), \quad d = x, y \quad (6)$$

and the weight function $w(\vec{r}_j - \vec{r}_i)$ is selected as

$$w(\vec{r}_j - \vec{r}_i) = \begin{cases} 1 - 6\bar{r}^2 + 8\bar{r}^3 - 3\bar{r}^4 & \bar{r} = \frac{r_{ij}}{R_e} = \frac{|\vec{r}_j - \vec{r}_i|}{R_e} \leq 1 \\ 0 & \bar{r} = \frac{r_{ij}}{R_e} = \frac{|\vec{r}_j - \vec{r}_i|}{R_e} > 1 \end{cases} \quad (7)$$

where \vec{r}_j and \vec{r}_i are the position vectors of neighbour and target particles, $r_{j,x}$ and $r_{j,y}$ are the component of \vec{r}_j in the x - and y - direction, R_e is the radius of the support domain proportional to Δl with Δl being the initial average particle distance and Δr_{ij} is defined as $\Delta r_{ij} = \max(0.8\Delta l, |\vec{r}_j - \vec{r}_i|)$.

The numerical value of β is very close 0 for inner particles and it rapidly increases when approaching to the interface or isolated particles. Although the gradient is theoretically infinite at the interface or isolated particles, it is just a large value in numerical computation.

To obtain a non-dimensional scale of the absolute density gradient β_0 is introduced with the expression of

$$\beta_0 = |\rho_1 - \rho_2|/\Delta l \quad (8)$$

where ρ_1 and ρ_2 are densities of two phases. The interface and isolated particles will be identified by the ratio of β/β_0 rather than the value of β . To shed some light on the order of the ratio, we may consider the special cases: uniformly distributed particles with some of them being on horizontal (or vertical) interface, diagonal interface or isolated. If only the nearest four neighbours are considered (i.e., the support domain is in the range of $1.0\Delta l$ and $\sqrt{2}\Delta l$), the value of β/β_0 should be 0.5 for horizontal or vertical interfaces, 1.0 for diagonal interfaces and 2.0 for isolated particles by using Eq. (5) and (6). It is noted here that for any distribution of particles with the weight function given by Eq. (7) and a fixed support domain size, the value of β/β_0 remains independent on the value of Δl . It is also noted that the value of β/β_0 will not be affected by the density ratio of the two phases. In

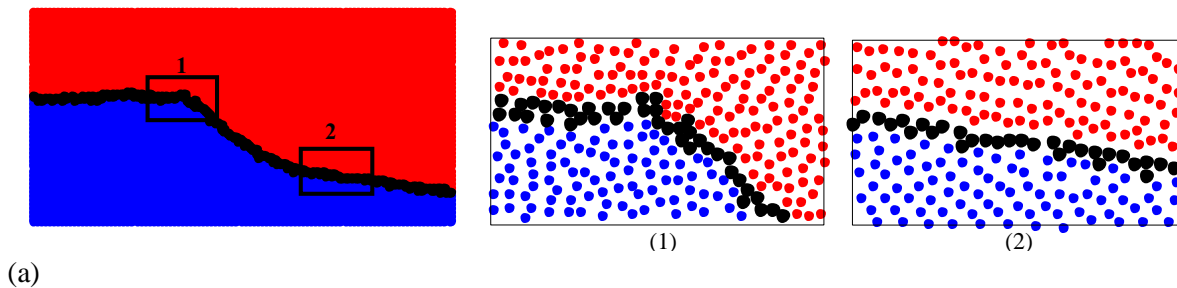
other words, the value of β/β_0 is independent on the total number of particles for a given domain and density ratio. Nevertheless, in general situations with the particular weight function used and the chosen radius of the support domain, the value of β/β_0 will vary in a range with the change of particle distribution. Therefore the most suitable values need to be determined by considering a range of flowing conditions of the two phases. The following two conditions (I) and (II) are then checked.

$$(I) \gamma < \beta/\beta_0 < \alpha \quad (9a)$$

$$(II) \beta/\beta_0 \geq \alpha \quad (9b)$$

If Condition (I) is satisfied, the particles are identified to be interface particles. If Condition (II) is met, the particles are identified as isolated particles. If none of the conditions is satisfied, they are classified as inner particles. For general cases, particles move and become irregularly distributed. The values of γ and α will be discussed below using numerical tests. This approach based on Eqs. (5) to (9) is shortened as ADG (absolute density gradient) method hereafter for convenience.

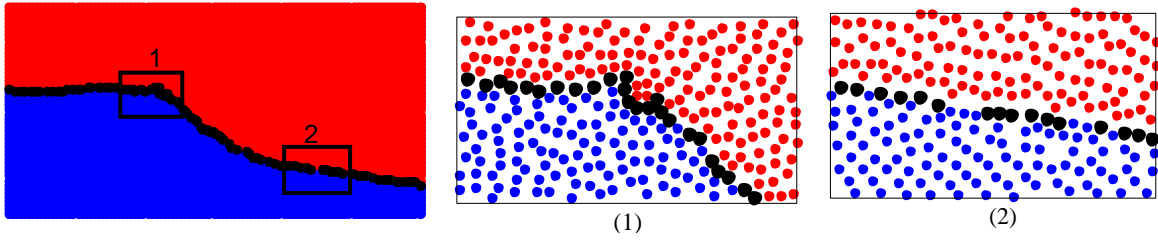
To determine the value of γ and α , a number of tests are carried out for a specified particle configurations shown in Figure 1. In this figure, two typical regions are enlarged. Particles are clustered in region 1 and relatively coarser in region 2. As shown in Figure 1(a), an under-specified value of γ (e.g. 0.1), leads to misidentifying inner particles close to the interface in the clustered region (some inner particles are identified as interface particles, i.e., over-identified). However, an over-specified value of γ (e.g. 0.5), shown in Figure 1(b), leads to missing the particles on the interface in the region where the distribution of particles is relatively coarser (i.e., under-identified). Based on this, we can deduce that there might be a range of values for γ which may lead to correctly identifying the interface particles. We have tested the value of γ in the range of 0.2 to 0.4 for the same configuration and found that the interface particles are correctly picked out and insensitive to the specific value in the range. The results of $\gamma = 0.2$ and $\gamma = 0.4$ are illustrated in Figure 2. Hereafter, the value of γ is selected to be 0.3, unless mentioned otherwise. It is noted here that the new scheme discussed above will not misidentify the inner particles away from interface as the value of β/β_0 is always zero or very close to zero for incompressible and weak compressible fluids. When the value of γ is smaller, it tends to be that more particles near the interface may be misidentified as interface particle (e.g., Figure 1a). However, this kind of misidentification will not significantly affect the computation results as the values of physical variables near the interface are very close to those on the interface. More discussions about this point may be found in Ma and Zhou (2009).



(a)

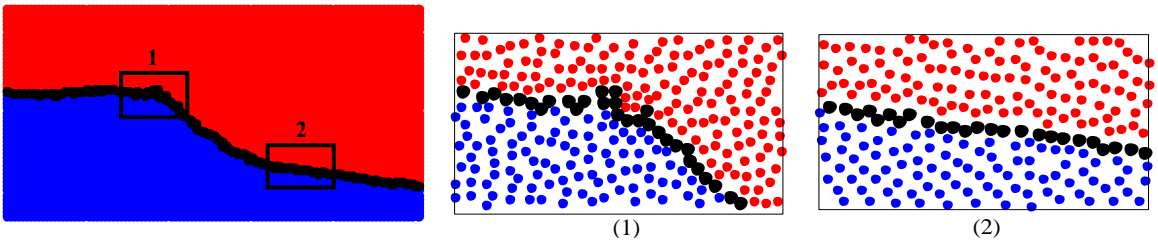
(1)

(2)

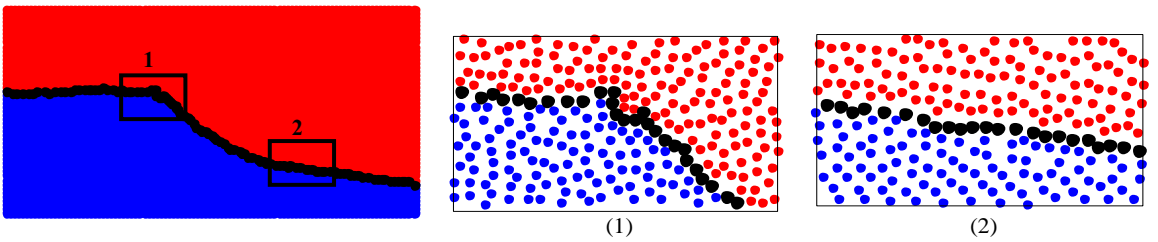


(b)

Figure 1: Examples of interface identifications when applying improper values of γ . (a) shows inner particles close to the interface are over-identified with $\gamma = 0.1$ and (b) shows some interface particles are under-identified with $\gamma = 0.5$. (density ratio: 1:1000)



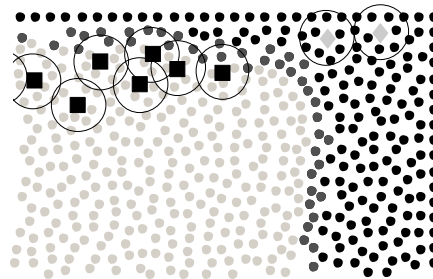
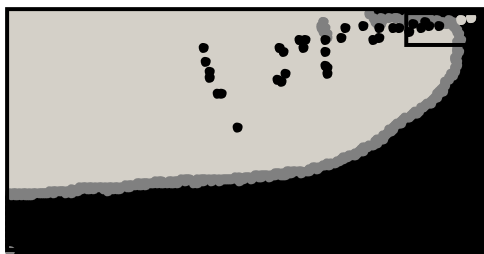
(a)



(b)

Figure 2: Examples of interface identifications when applying proper values of γ . (a) shows the interface identified by $\gamma = 0.2$ and (b) is obtained by $\gamma = 0.4$. (density ratio: 1:1000)

Another particle configuration associated with the violent sloshing of two phases is used to illustrate the effects of value for α in Condition (II). Figure 3(a) and (b) show that the isolated particles penetrating into the other phase are identified by using the value of α to be 1.4 and 1.6, respectively. It can be seen that the isolated particles of both phases are correctly identified by using either value. This demonstrates that the results are not sensitive to the value of α when it is within the range of 1.4 to 1.6. Thus $\alpha=1.5$ will be used for isolated particle identification.



(a)

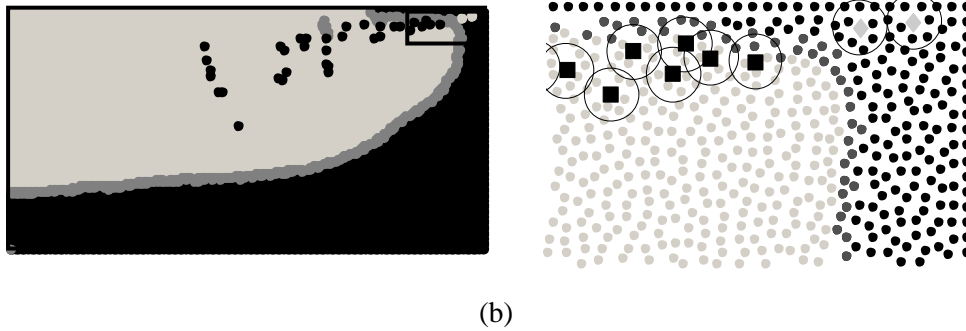


Figure 3: Isolated particles marked by squares for heavier fluid particles and diamonds for lighter fluid particles (density ratio: 1:1000) are identified with α being 1.4 (a) and 1.6 (b). The heavier phase is marked in black and the lighter is in light grey. In the enlarged figures on the right, support domains for each isolated particles are marked with a circle.

According to above numerical tests, the values of γ and α are selected to be 0.3 and 1.5 for the conditions of (I) and (II) to identify the interface particles and isolated particles, respectively.

4 Validations

4.1 Identification with different random distributions of particles

The newly proposed interface identification technique will be further validated on random distributed particles. Comparison will be made with the results of other two methods. One is the PND method used by SPH simulation and the other is the MPAM suggested by Ma & Zhou (2009) as mentioned in Section 2. The tests are first carried out on the specified configuration shown in Figure 4 in which the unit patch is divided into two portions by a sinusoidal curve of $y = 0.1\sin(2\pi x) + 0.5$. Particles are randomly distributed by using the ‘haltonset’ function available in MATLAB. Below the sinusoidal curve the particles represent the fluid phase 1 (blue dots) and the rest is filled by fluid phase 2 (red dots).

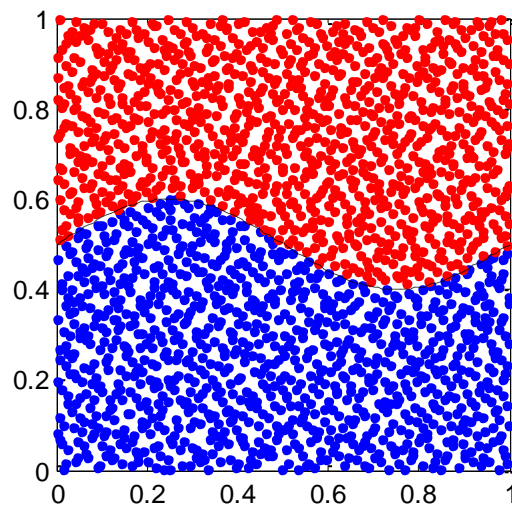


Figure 4: Sketch of interface testing case. 2000 random distributed particles in a unit patch divided into two portions by $y = 0.1\sin(2\pi x) + 0.5$ shown by dashed line. Blue and red dots represent the fluid phase 1 and fluid phase 2, respectively.

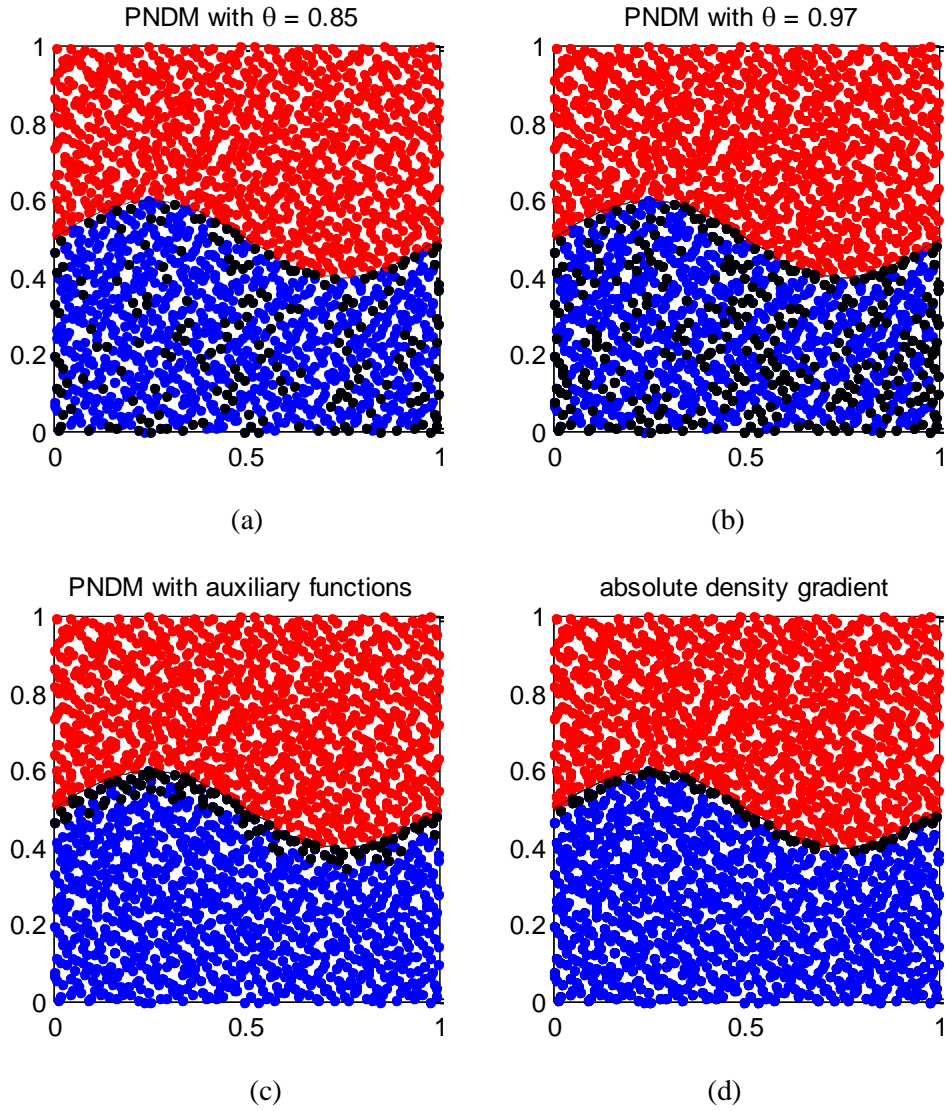


Figure 5: Interface particles (black nodes) identification by PND with $\theta = 0.85$ (a), PND with $\theta = 0.97$ (b), PND with auxiliary functions (c) and ADG (d).Blue and red dots represent the fluid phase 1 and fluid phase 2 respectively.(density ratio=0.9)

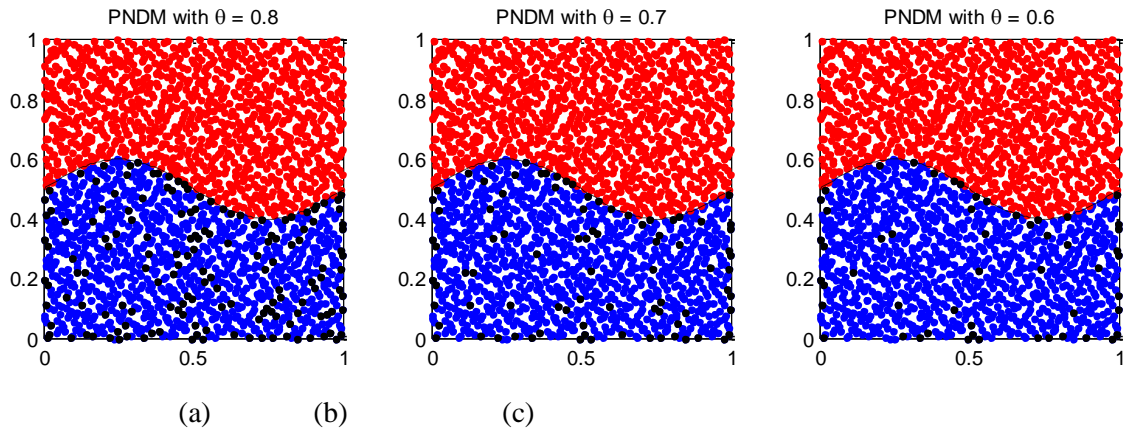


Figure 6: Interface particles (black nodes) identification by PND with $\theta = 0.8$ (a), $\theta = 0.7$ (b) and $\theta = 0.6$ (c). Blue and red dots represent the fluid phase 1 and fluid phase 2, respectively.

When using the PND and MPAM methods, interface particles are identified as surface particles of the phase 1 by ignoring the present of the phase 2 as they are developed for single phase problem. As shown in Figure 5 black dots are interface particles identified by the PND method with $\theta = 0.85$ and

$\theta = 0.97$ in Figure 5(a) and (b), which are in the range of θ proposed by (Koshizuka & Oka 1996). One can observe that the interface particles are highly over-identified as many inner particles are marked as interface ones although it is moderately relieved by decreasing the coefficient. Such over-identification was also observed by (Zheng et al. 2014) in their dam breaking simulation. There are also several particles located on the interface but not identified by using either value of θ . Other θ values are also tested and the results are shown in Figure 6. One can find that decreasing the value helps alleviate over-identification of inner particles but more interface particles are also missed. The reasons for such inaccuracy are that the accuracy of the PND method strongly depends on the randomness of the particle distribution which was pointed out by (Ma & Zhou 2009). For inner particles, coarse distribution leads to low particle number density even with a complete support domain and so over-identification happens. On the contrast, particles clustering on the interface leads to high particle number density even though the support domain of its own phase is incomplete, leading to their misidentification to inner particles. For the results obtained using the MPAM shown in Figure 5(c), the accuracy is significantly improved. But over-identification still happens on inner particles close to the interface. Since this identification technique is based on the interface particles identified at the previous time step, error accumulation may occur after long time simulation. Figure 5(d) shows the results obtained by the method proposed in this paper. It can be seen that almost all the interface particles are correctly identified. No inner particles are wrongly identified by the method. As indicated above, the new technique does not depend on the density ratio. To confirm this, the tests are also carried out on different density ratios of 0.1 and 0.01 in addition to the ratio of 0.9 in Figure 5(d) by using the ADG method, and the results for the density ratios of 0.1 and 0.01 are shown in Figure 7. This figure and Figure 5(d) show that the accurate identification is achieved in all the cases, demonstrating that the ADG method results are independent of the density ratios.

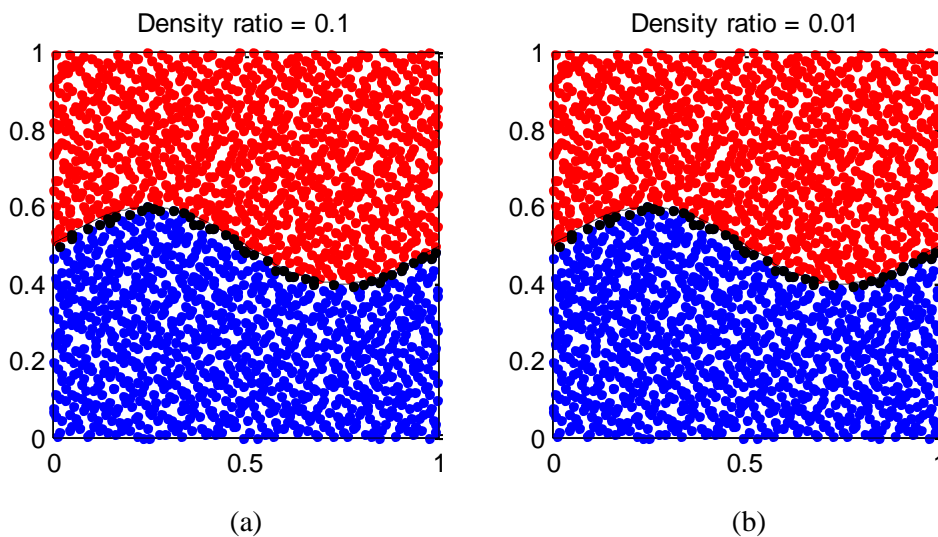


Figure 7: Interface particles (black nodes) identification by ADG technique on density ratios of 0.1 with the densities of blue and red dots of 10 and 1 respectively in (a) and 0.01 with the densities of blue and red dots of 100 and 1 respectively in (b).

In modelling violent multiphase flow, the particle distribution can become very random even they are uniformly distributed initially. It is important that the behaviours of interface identification methods should be examined for different levels of randomness of particle distributions. For this purpose, we use a configuration similar to that in Figure 4 with particle number of 2500; however the particles are distributed in a way that they are first uniformly located and then deviated by $\Delta\vec{r} = k \left[(R_{n_x} -$

$0.5)\vec{e}_x + (R_{n_y} - 0.5)\vec{e}_y]\Delta l$, i.e., the position of particle is given by $\vec{r} = \vec{r}_0 + \Delta\vec{r}$ where each of R_{n_x} and R_{n_y} is a group of random numbers ranging from 0 to 1.0 generated separately in x - and y -direction, respectively; k is the randomness coefficient and Δl is the particle distance in uniform distribution; \vec{e}_x and \vec{e}_y are the unit vector in x - and y -direction, respectively; $k = 0$ leads to zero deviation and uniform distribution. As k increases, the distribution becomes more disorderly. If the value of k is equal to or large than 1, there would be possibility that the position of a particle can be shifted by more than Δl . The three methods (PND, MPAM and ADG) are employed to identify the interface particles for the cases with different level of randomness. The numbers of particles inaccurately identified for three techniques are listed in Table 1 with k increasing from 0 to 1.2. The reference number is the number of particles on the interface, which are at or near the specified interface curve within the distance of $0.5\Delta l$. One can see that the number of misidentified particles by the PND method is small only when the value of k is very small but with the increase of the k value (level of randomness), the number of misidentified particles are large, even much larger than the number of interface particles. In contrast, the number of misidentified particles for each value of k by the MPAM is significantly reduced but is still considerable. Comparatively, the number of misidentification by the ADG method is very small and not increases with the increase of randomness. To have a clearer look at their performances, the ratio of inaccurate identification defined as the number of misidentified particles divided by the reference number is demonstrated in Figure 8. It shows that, by increasing the randomness, more than 7 times of the interface particles are misidentified by the PND when k reaches 1.2 while this ratio decreases to 0.97 with more moderate incensement by the MPAM. The maximum ratio is only 0.125 arising at $k = 1.0$ and shows less dependency on the value of k by the ADG. With the same configuration, the total particle numbers of 900, 1600, 2500, 3600, 4900 and 6400 are also tested using the ADG method with the values of $k = 0.6, 0.8, 1.0$ and 1.2 . The results are given in Figure 9, showing that the performance of the ADG technique is insensitive to the particle number. This observation is consistent with what is mentioned previously that the technique does not depend on the average distance between particles. The slight change in the results showing in Figure 9 is due to random distribution of particles.

Table 2: The number of misidentified particles for different particle distribution randomness by using PND, MPAM and ADG methods

Randomness k	Reference No.*	Number of misidentified particles		
		PND	MPAM	ADG
0	37	0	2	0
0.2	42	54	16	0
0.4	40	173	17	0
0.6	37	222	22	1
0.8	36	232	30	3
1.0	32	222	30	2
1.2	33	232	32	1

Reference No.* is the number of particles at or near the specified interface curve within the distance of $0.5\Delta l$ for different randomness of k

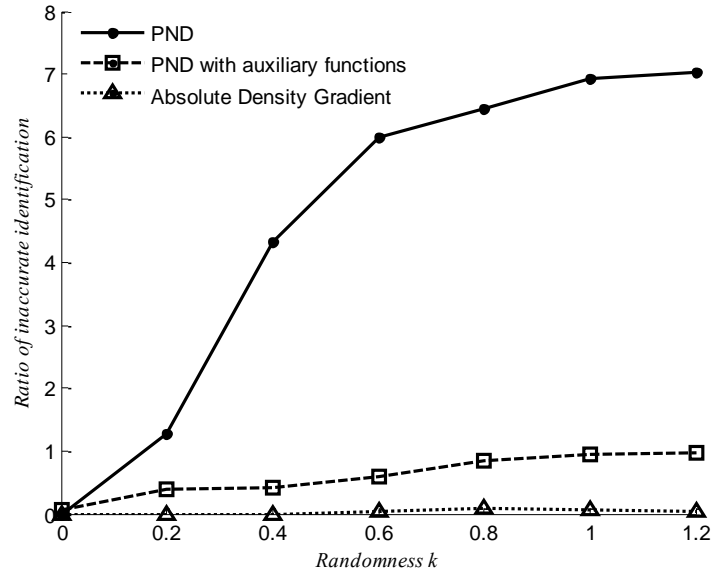


Figure 8: The ratios of inaccurate identification (number of misidentified particles/the reference number) of increasing randomness by using three identification techniques.

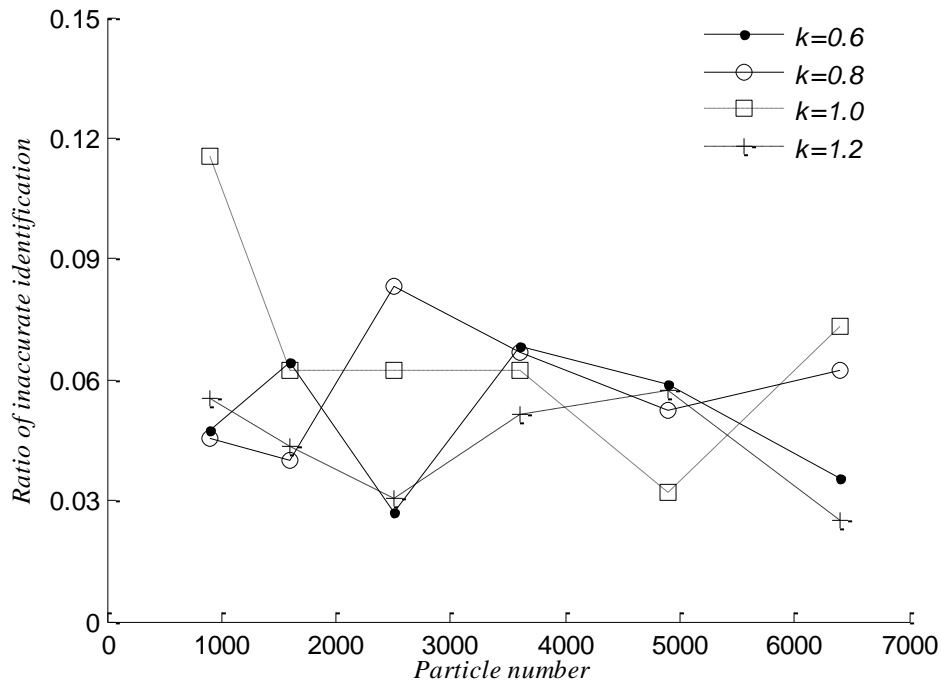


Figure 9: The ratios of inaccurate identification (number of misidentified particles/the reference number) of increasing total particle number using the method of ADG with randomness coefficients of 0.6 and 0.8

Tests are also carried out for various support domain sizes R_e of the weight function within the range of $1.4\Delta l$ to $4.0\Delta l$ which is widely adopted for function interpolation, gradient and Laplacian approximations (Ataie-Ashtiani & Farhadi 2006; Gotoh & Fredsøe 2000; Xu & Jin 2014; Zheng et al.

2014). Following the above setup for $k = 0.6$ and 1.0 , the numbers of misidentified particles by the ADG are listed in Table 2. It shows that small support domain (e.g. $R_e/\Delta l = 1.4$ and 1.6) leads to moderate increment of misidentification due to insufficient neighbouring particles to accurately estimate the density gradient. By increasing $R_e/\Delta l (>2.1)$, the results become insensitive to the variation of the size and even better. Considering the computational time, $R_e/\Delta l = 2.1$ as selected in above tests is reasonable, but one can choose to use a larger support domain for identifying the interface particles.

Table 3: Numbers of misidentified particles by the ADG method with different support domain size R_e for two values of $k = 0.6$ and 1.0

$R_e/\Delta l$	1.4	1.6	1.8	2.1	2.5	3.0	3.5	4.0
$k = 0.6$	7	6	2	1	0	0	0	0
$k = 1.0$	8	6	3	2	1	1	0	0

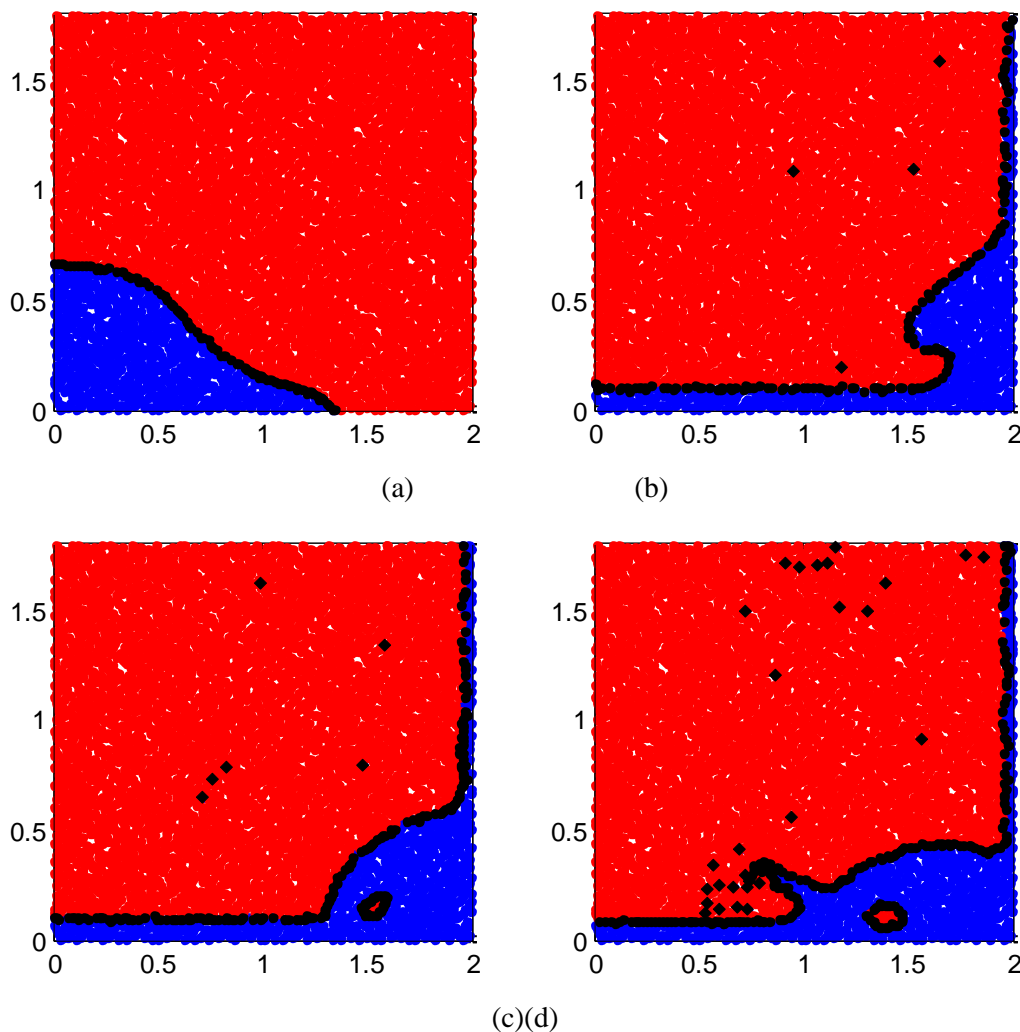


Figure 10: Black dots and filled diamonds are interface and isolated particles identified by the ADG technique in four dam breaking snapshots. The heavier fluid with the density of 1.0 of phase 1 is represented by blue dots and the lighter fluid with density of 0.001 of phase 2 is represented by red dots.

4.2 Identifications for the dam breaking flow

To further validate the newly proposed identification technique on different flow conditions, four snapshots are picked from a dam breaking simulation (Zheng et al. 2014), in which the heavier fluid

(phase 1-water) indicated by blue dots is released in the lighter fluid (phase 2 – air) indicated by red dots. The four configurations shown in Figure 10 include the changing and irregular shape of the released water with a smooth interface in (a), a backward jet in (b), the jet merging into the bottom water in (c) and a second jet in (d). A trapped air bubble also appears in (c) and (d). The density ratio of the two phases in this test is 1:1000. As we can observe from Figure 10, the interface and isolated particles (black dots) are accurately identified for all the configurations, indicating that the ADG method works well for the more complex cases.

5 Conclusion

This paper presents a new interface particle identification method for two-phase flows based on the absolute density gradient (ADG). The behaviour of the method is tested for different configurations including these with different level of randomness. It is shown that the accuracy of the method is independent of the density ratio of two phases and of the average distance between particles. In all the cases tested, the method can correctly pick up almost all the interface and isolated particles as long as the support domain is larger than twice average distance of particles.

Acknowledgement

The authors gratefully acknowledge the PhD scholarship provided to Y Zhou by City University and China Scholarship Council and the financial support of the EPSRC through a research grant (EP/L01467X/1).

References

- Ataie-Ashtiani, B. & Farhadi, L., 2006. A stable moving-particle semi-implicit method for free surface flows. *Fluid Dynamics Research*, 38(4), pp.241–256.
- Aulisa, E. Manservigi, S. Scardovelli, R. & Zaleski, S., 2007. Interface reconstruction with least-squares fit and split advection in three-dimensional Cartesian geometry. *Journal of Computational Physics*, 225(2), pp.2301–2319.
- Ausas, R.F., Dari, E.A. & Buscaglia, G.C., 2011. Arterial fluid mechanics modeling with the stabilized space – time fluid – structure interaction technique. *A geometric mass-preserving redistancing scheme for the level set function*, 65, pp.989–1010.
- Chen, Z. Zong, Z. Liu, M.B. Zou, L. Li, H.T. & Shu, C., 2015. An SPH model for multiphase flows with complex interfaces and large density differences. *Journal of Computational Physics*, 283, pp.169–188.
- Diwakar, S. V., Das, S.K. & Sundararajan, T., 2009. A Quadratic Spline based Interface (QUASI) reconstruction algorithm for accurate tracking of two-phase flows. *Journal of Computational Physics*, 228(24), pp.9107–9130.

- Ginzburg, I. & Wittum, G., 2001. Two-Phase Flows on Interface Refined Grids Modeled with VOF, Staggered Finite Volumes, and Spline Interpolants. *Journal of Computational Physics*, 166(2), pp.302–335.
- Gotoh, H. & Fredsøe, J., 2000. Lagrangian Two-Phase Flow Model of the Settling Behavior of Fine Sediment Dumped into Water. *Coastal Engineering*, (1997), pp.3906–3919.
- Gotoh, H. & Sakai, T., 2006. Key issues in the particle method for computation of wave breaking. *Coastal Engineering*, 53(2-3), pp.171–179.
- Hirt, C.W. & Nichols, B.D., 1981. Volume of fluid (VOF) method for the dynamics of free boundaries. *Journal of Computational Physics*, 39(1), pp.201–225.
- Hoang, D.A. Steijn, Volkert van, Portela, Luis M. Kreutzer, Michiel T. & Kleijn, Chris R., 2013. Benchmark numerical simulations of segmented two-phase flows in microchannels using the Volume of Fluid method. *Computers and Fluids*, 86, pp.28–36.
- Hu, X.Y. & Adams, N. a., 2007. An incompressible multi-phase SPH method. *Journal of Computational Physics*, 227(1), pp.264–278.
- Khayyer, a. & Gotoh, H., 2013. Enhancement of performance and stability of MPS mesh-free particle method for multiphase flows characterized by high density ratios. *Journal of Computational Physics*, 242, pp.211–233.
- Koshizuka, S., Nobe, A. & Oka, Y., 1998. Numerical analysis of breaking waves using the moving particle semi-implicit method. *International Journal for Numerical Methods in Fluids*, 26(7), pp.751–769.
- Koshizuka, S. & Oka, Y., 1996. Moving-particle semi-implicit method for fragmentation of incompressible fluid. *Nuclear science and engineering*, 123(3), pp.421–434.
- Lee, E.S. Moulinec, C. Xu, R. Violeau, D. Laurence, D. & Stansby, P., 2008. Comparisons of weakly compressible and truly incompressible algorithms for the SPH mesh free particle method. *Journal of Computational Physics*, 227(18), pp.8417–8436.
- Lind, S.J. Xu, R. Stansby, P. K. & Rogers, B.D., 2012. Incompressible smoothed particle hydrodynamics for free: surface flows: A generalised diffusion-based algorithm for stability and validations for impulsive flows and propagating waves. *Journal of Computational Physics*, 231(4), pp.1499–1523.
- López, J. Hernández, J. Gómez, P. & Faura, F., 2004. A volume of fluid method based on multidimensional advection and spline interface reconstruction. *Journal of Computational Physics*, 195(2), pp.718–742.
- Ma, Q.W., 2008. A New Meshless Interpolation Scheme for MLPG_R Method. *CMES - Computer Modeling in Engineering and Sciences*, 23(2), pp.75–89.
- Ma, Q.W., 2005. MLPG Method Based on Rankine Source Solution for Simulating Nonlinear Water Waves. *CMES - Computer Modeling in Engineering and Sciences*, 9(2), pp.193–209.

- Ma, Q.W. & Zhou, J.T., 2009. MLPG_R Method for Numerical Simulation of 2D Breaking Waves. *CMES - Computer Modeling in Engineering and Sciences*, 43(3), pp.277–303.
- Min, C., 2010. On reinitializing level set functions. *Journal of Computational Physics*, 229(8), pp.2764–2772.
- Muzaferija, S. & Perić, M., 1997. Computation of Free-Surface Flows Using the Finite-Volume Method and Moving Grids. *Numerical Heat Transfer, Part B: Fundamentals*, 32(4), pp.369–384.
- Osher, S. & Sethian, J. a., 1988. Fronts propagating with curvature dependent speed: Algorithms based on Hamilton-Jacobi formulations. *Journal of Computational Physics*, 79, pp.12–49.
- Rafiee, A. Cummins, S. Rudman, M. & Thiagarajan, K., 2012. Comparative study on the accuracy and stability of SPH schemes in simulating energetic free-surface flows. *European Journal of Mechanics, B/Fluids*, 36, pp.1–16.
- Renardy, Y. & Renardy, M., 2002. PROST: A Parabolic Reconstruction of Surface Tension for the Volume-of-Fluid Method. *Journal of Computational Physics*, 183(2), pp.400–421.
- Rudman, M., 1997. Volume-Tracking Methods for Interfacial Flow Calculations. *International Journal for Numerical Methods in Fluids*, 24(7), pp.671–691.
- Shakibaenia, A. & Jin, Y.C., 2012. Lagrangian multiphase modeling of sand discharge into still water. *Advances in Water Resources*, 48, pp.55–67.
- Shao, S.D., 2012. Incompressible smoothed particle hydrodynamics simulation of multifluid flows. *International Journal for Numerical Methods in Fluids*, 69, pp.1715–1735.
- Shao, S.D., 2009. Incompressible SPH simulation of water entry of a free-falling object. *International Journal for Numerical Methods in Fluids*, 59, pp.59–115.
- Sussman, M. & Fatemi, E., 1999. An Efficient, Interface-Preserving Level Set Redistancing Algorithm and Its Application to Interfacial Incompressible Fluid Flow. *SIAM Journal on Scientific Computing*, 20(4), pp.1165–1191.
- Tukovic, Z. & Jasak, H., 2012. A moving mesh finite volume interface tracking method for surface tension dominated interfacial fluid flow. *Computers and Fluids*, 55, pp.70–84.
- Ubbink, O. & Issa, R.I., 1999. A Method for Capturing Sharp Fluid Interfaces on Arbitrary Meshes. *Journal of Computational Physics*, 153(1), pp.26–50.
- Weller, H.G., 2008. A New Approach to VOF-based Interface Capturing Methods for Incompressible and Compressible Flow. *Technical Report TR/HGW/07, OpenCFD Ltd.*, (May).
- Xiao, F., Honma, Y. & Kono, T., 2005. A simple algebraic interface capturing scheme using hyperbolic tangent function. *International Journal for Numerical Methods in Fluids*, 48(9), pp.1023–1040.
- Xu, T. & Jin, Y.-C., 2014. Numerical investigation of flow in pool-and-weir fishways using a meshless particle method. *Journal of Hydraulic Research*, 52(6), pp.849–861.
- Yokoi, K., 2007. Efficient implementation of THINC scheme: A simple and practical smoothed VOF algorithm. *Journal of Computational Physics*, 226(2), pp.1985–2002.

Zhang, Y., Zou, Q. & Greaves, D., 2010. Numerical simulation of free-surface flow using the level-set method with global mass correction. *International Journal for Numerical Methods in Fluids*, 63, pp.651–680.

Zheng, X., Ma, Q.W. & Duan, W.Y., 2014. Incompressible SPH method based on Rankine source solution for violent water wave simulation. *Journal of Computational Physics*, 276, pp.291–314.